



Research Article

Numerical investigation into the effect of duct use on the performance of controllable pitch propellers

Ahmet YURTSEVEN*

Department of Marine Engineering, Yıldız Technical University, Faculty of Naval Architecture and Maritime, İstanbul, Türkiye

ARTICLE INFO

Article history

Received: May 27, 2023

Revised: September 11, 2023

Accepted: October 03, 2023

Key words:

CFD; CPP; duct; ducted propeller; spindle torque

ABSTRACT

This study uses CFD methods to solve the complex flow around a CPP propeller with ducts and aims to investigate the performance differences between ducted and non-ducted propeller designs. In particular, the values for pitch changes and blade spindle torques have been determined at different advance ratios. The study uses STAR-CCM+, a commercial computational fluid dynamics (CFD) code, and has preferred the k- ϵ model to predict turbulence in the flow. In addition to the thrust coefficient, torque coefficient, and propeller efficiency, the study also examines blade spindle torque, which provides movement to the propeller blades. The use of ducts at low advance ratios is found to be beneficial in terms of both improving performance and reducing torque.

Cite this article as: Yurtseven A. Numerical investigation into the effect of duct use on the performance of controllable pitch propellers. *Seatific* 2023;3:2:43–50.

1. INTRODUCTION

Propeller efficiency is the most important parameter affecting propulsion system efficiency in marine vessels. One of the methods applied to increase propeller efficiency is to change the pitch angles of the propeller blades based on vehicle speed while keeping propeller speed constant. Propellers that can perform this maneuver are called controllable pitch propellers (CPP). Another application is to make the propellers work within a non-movable nozzle (duct). These types of propellers are called ducted propellers.

Two types of ducted propeller structures are often used on ships (Celik et al., 2011). The first is the accelerating ducted propeller system that accelerates the flow on heavily loaded and diameter-restricted propellers, and the second is the decelerating ducted propeller system, which increases static pressure by slowing down the flow over the propeller to delay propeller cavitation. System efficiency has been

observed to increase with the additional loading of the duct in ducted propellers. However, the additional loading of the duct is limited to the current separation at the duct. Propellers with current accelerating ducts are generally used in tug-like vessels that perform pushing and pulling operations. They are also preferred on research vessels, drilling platforms, and marine vessels that require the ability to hold position (Oosterveld, 1972).

Trawlers also use ducted propellers due to the need for a high thrust ratio at a low advance ratio. Methods based on computational fluid dynamics (CFD) can be used for the design and operating parameters of ducted propellers used in these types of boats (Caldas et al., 2019). Some studies are found in the literature on ducted propellers (Bhattacharyya et al., 2015, 2016b; Baltazar et al., 2019; Zhang et al., 2019, 2020; Gong et al., 2021; Zhang et al., 2021; Kim et al., 2022). Celik et al. (2010) developed an iterative design methodology for ducted propellers due

*Corresponding author.

*E-mail address: ahmety@yildiz.edu.tr, yurtseven1@gmail.com



to the insufficient accuracy of classical propeller design methods under heavy loading conditions. Haimov et al. (2011) used several different types of ducts to obtain the combined effect of the Reynolds number and loading on thrust and torque by comparing model and full-scale calculations in turbulent flow, confirming the characteristics and efficiency gains of ducted propellers.

Ducts can be used with fixed pitch propellers as well as with controllable pitch propellers. In particular, the ability to change pitch in case of current separation, which can cause a decrease in thrust, has shown better characteristic values in controllable pitch propellers than in fixed pitch propellers (Elbatran et al., 2014). Very few ducted CPP propeller studies are found in the literature (Arief et al., 2021; Huisman et al., 2022). Panel methods working with potential theory have been used to analyze the performance of CPP propellers with nozzles. However, Liu et al. (2006) realized that viscous solutions should be used for torque values in particular.

Scaling effects are also found among studies. The scaling effects of both propellers and ducts have been investigated with regard to performance. Scaling effects were found to have a greater effect on the thrust from ducts than on propeller characteristics. The effect of the design and scale of the ducts on thrust with current separation has been shown to be significant at high advance ratios. Much better results were obtained in the full-scale analysis of ducted propellers compared to scale models (Bhattacharyya et al., 2016a).

The operating procedures for CPP propellers require the blades to be rotated around their axis to change the pitch angle. This introduces the concept of spindle torque, which is not present in fixed-pitch propellers. A few studies are also found in the literature on the propeller blade spindle torque of CPP propellers (Godjevac et al., 2009; Jessup et al., 2009; Martelli et al., 2013; Tarbiat et al., 2014; Pourmostafa et al., 2021; Yurtseven et al., 2023). Determining blade spindle torques is also very important for aiding the design of CPP propellers and for avoiding excessive blade actuation pressures at the blade hub (Liu et al., 2015). The torque on the blade can be investigated numerically using potential theory verified by a simulation. Studies should also clearly analyze well the complex flow conditions around CPP propeller blades (Funeno et al., 2013).

This study uses CFD methods to analyze the complex flow around a ducted CPP propeller and aims to investigate the performance differences between ducted and non-ducted propeller designs. In particular, the values for pitch change and blade spindle torque have been determined at different advance ratios.

2. NUMERICAL MODELING

2.1. Governing equations

The analyses using computational fluid dynamics methods model the flow as three-dimensional, steady state, viscous, turbulent, and incompressible. This study has preferred the realizable k-epsilon turbulence model,

with the continuity and steady state Reynolds averaged Navier-Stokes equations being as follows:

$$\frac{\partial U_i}{\partial x_i} = 0 \quad (1)$$

$$pU_j \frac{\partial U_i}{\partial x_j} = -\frac{\partial P}{\partial x_i} + \frac{\partial \tau}{\partial x_j} - \frac{\partial (\overline{pu'_i u'_j})}{\partial x_i} \quad (2)$$

where U_i is the average velocity vector, u' is the turbulence velocity vector, $\overline{pu'_i u'_j}$ is the turbulence stress tensor, P is average pressure, ρ is density, and μ is dynamic viscosity. The study uses Simcenter Star CCM+ version 2020.3, a commercial CFD code. The solver applies the finite volume method to discretize the governing equations.

Both spatial and temporal discretization has been done with accurate second-order schemes to improve accuracy. The well-known SIMPLE algorithm is used for pressure-velocity matching. More information about the numerical solution can be found in the solver manual (Siemens, 2021).

Figure 1 shows a flow stream volume to represent the flow around the propeller. The dimensions in the figure are defined based on propeller diameter. The following conditions have been defined: uniform velocity inlet for the inlet surface, pressure outlet for the outlet surface, symmetry at the side surface, and no-slip for all other surfaces. This study was carried out by conducting analyses under open water propeller test conditions. As shown in Figure 2, propeller pitch changes

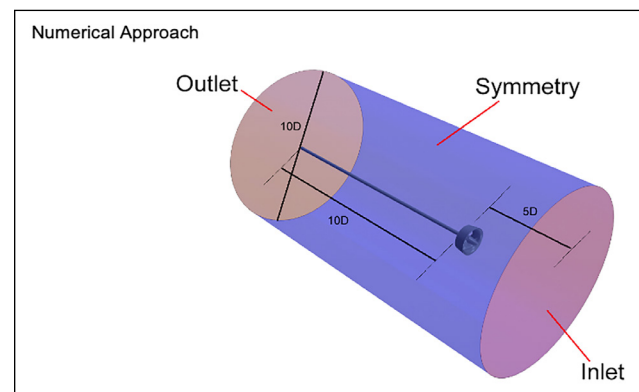


Figure 1. Solution volume and boundary types.

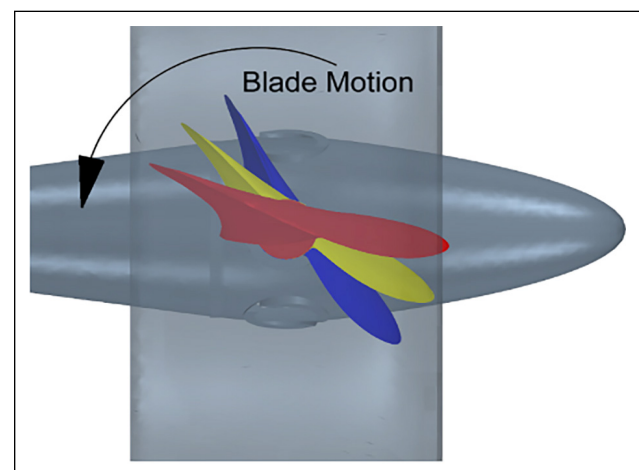


Figure 2. Propeller blade movement for changing pitch.

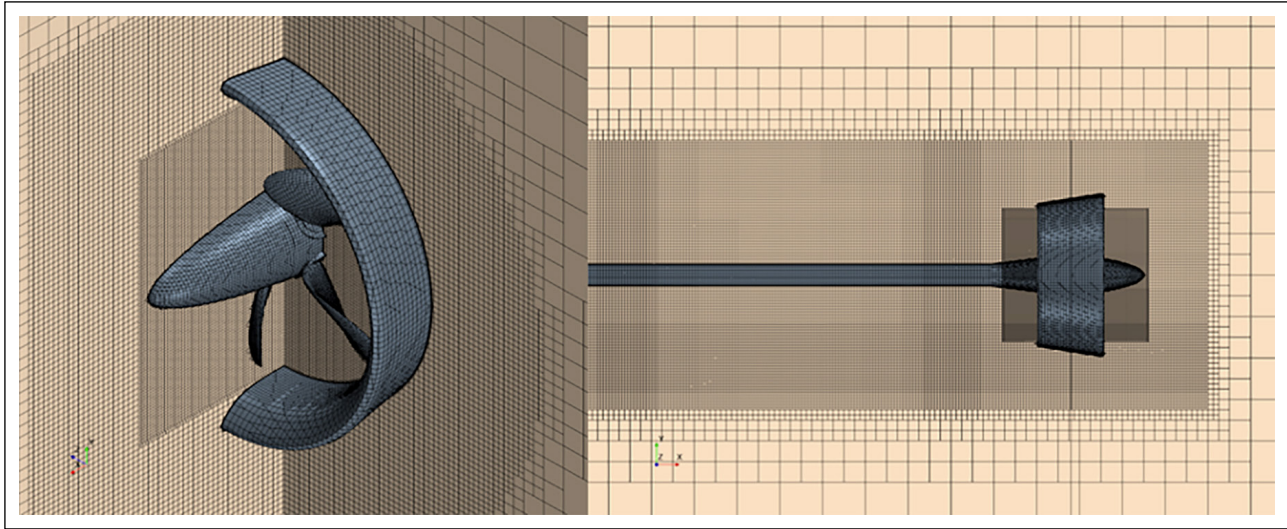


Figure 3. Detailed view of the solution grid.

were achieved through maneuvers that were obtained by rotating the propeller blades around the shaft axis.

CPP propellers'ability to change pitch angle (unlike FPP propellers) as well as to rotate around the main drive shaft also requires the blades to rotate around their own spindle axis. This leads to the need for an additional motion model in simulations. This study uses the motion reference frame for the propeller's main rotational motion. Although the overset motion model needed to be used for pitch changes, each pitch angle was generated and analyzed sequentially due to the simulations being run independently of time.

2.2. Grid structure

In order to analyze the solution volume using the finite volume method, a solution mesh consisting of unstructured hexahedral mesh elements was generated as shown in Figure 3.

Solution element refinement zones were designed for the propeller blades, shaft, hub, and duct based on the solution mesh. Prism layer elements are used close to the surfaces for accurate estimation of high-speed gradients.

2.3. Verification study

Roache's (1994) solution grid convergence index (GCI) method was used to determine the numerical uncertainty in the simulation studies. GCI is based on the Richardson extrapolation method, which estimates the exact numerical solution to be obtained using a zero-dimensional solution element through systematically obtained solution mesh results. GCI is also recommended by the American Society of Mechanical Engineers (ASME; Celik et al., 2008), International Towing Tank Conference (ITTC, 1999), and American Institute of Aeronautics and Astronautics (AIAA; Cosner et al., 2006) for numerical uncertainty assessments (Kim et al., 2021).

This study performed GCI by generating the solution mesh at three different resolutions. The basic size of the solution mesh elements were determined as shown by Equation 3.

$$h = \left[\frac{1}{N} \sum_{i=1}^N (\Delta V_i) \right]^{1/3} \quad (3)$$

where N is the number of solution elements, ΔV_i is the volume of each solution element, and h is the basic dimension. For the three different solution mesh resolutions (i.e., fine, medium, and coarse), the basic dimensions are h_1 , h_2 and h_3 respectively. Refinement factors are taken as $r_{21}=h_2/h_1$, $r_{32}=h_3/h_2$. The equations used for calculating the GCI are as follow:

$$\varepsilon_{32} = \varphi_3 - \varphi_2, \quad \varepsilon_{21} = \varphi_2 - \varphi_1 \quad (4)$$

where the φ values indicate the result of the analysis at each mesh resolution.

$$p = \frac{1}{\ln(r_{21})} |\ln|\varepsilon_{32}/\varepsilon_{21}| + q(p)| \quad (5)$$

$$q(p) = \ln \left(\frac{r_{21}^p - S}{r_{32}^p - S} \right) \quad (6)$$

$$S = 1. \text{sgn}(\varepsilon_{32}/\varepsilon_{21}) \quad (7)$$

The p value indicates the order value of the GCI method that is used.

$$\varphi_{ext}^{21} = (r_{21}^p \varphi_1 - \varphi_2) / (r_{21}^p - 1) \quad (8)$$

Table 1. Results from the GCI study (J=0.16)

	Value
N_1	8713836
N_2	4477850
N_3	2322435
ϕ_1	0.870
ϕ_2	0.864
ϕ_3	0.849
p	15.150
ϕ_{ext}^{21}	0.870
e^{21}	0.0069
e_{ext}^{21}	0.00018
$GCI_{fine}^{21} (\%)$	0.023

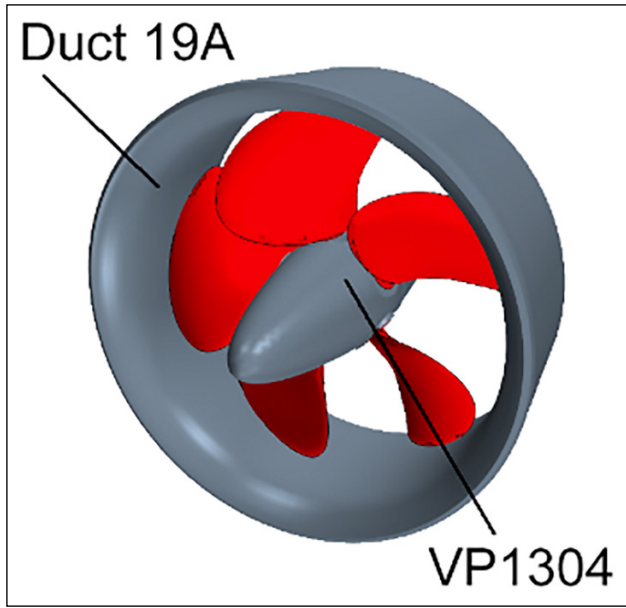


Figure 4. The VP1304 propeller and Duct 19A duct geometry.

$$e_a^{2l} = \left| \frac{\varphi_1 - \varphi_2}{\varphi_1} \right| \quad (9)$$

$$e_{ext}^{2l} = \left| \frac{\varphi_{ext}^{12} - \varphi_1}{\varphi_{ext}^{12}} \right| \quad (10)$$

$$GCI_{fine}^{2l} = \frac{1.25e_a^{2l}}{r_{2l-1}^p} \quad (11)$$

The sub-index *ext* here indicates the exact value. Table 1 shows the results from the GCI study, with N indicating the number of cells, φ indicating the coefficient of thrust, and e indicating the error quantities. Thus, the solution grid was determined to be needed at a medium resolution for the analysis.

2.4. Problem description

2.4.1. Geometry

The study uses the 5-blade CPP test propeller VP1304 as shown in Figure 4 together with Duct 19A, a standard duct frequently encountered in the literature.

The geometric dimensions and details are given in Table 2.

2.5. Validation study

Figure 5 shows the comparison of the experimental data obtained under open water propeller test conditions with the results from the numerical study.

According to the data obtained at six different advance ratios, the results from the numerical study are understood to show good agreement with the experimental results.

Table 2. Geometric details of the VP1304 propeller

D	0.250 m
Blade number	5
Rotation direction	Right
$P_{0.7}/D$	1.635
Propeller Shaft	Downstream

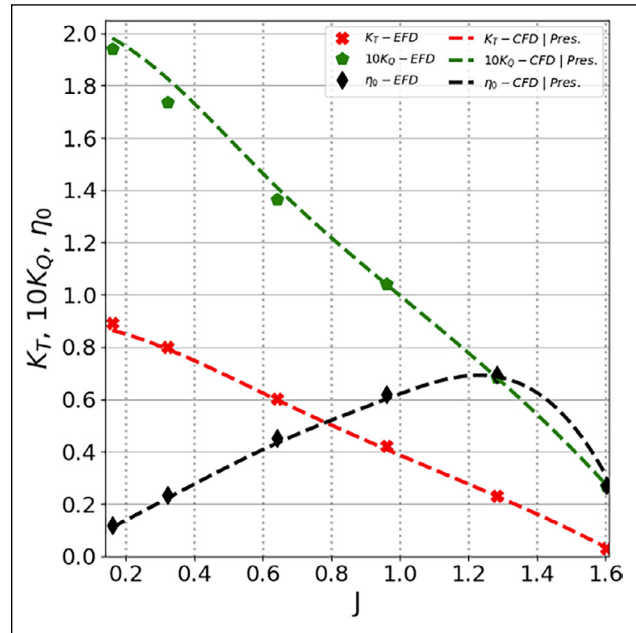


Figure 5. Experimental and numerical study results for the VP1304 propeller (Heinke, 2011).

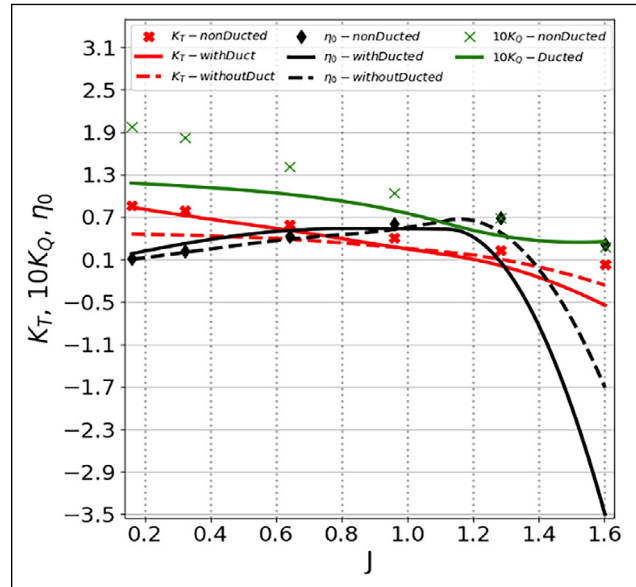


Figure 6. Performance coefficients for the ducted and non-ducted VP1304 CPP.

CPP: Controllable pitch propellers.

3. RESULTS

This section presents the numerical simulation results for the VP1304 test propeller and Duct 19A duct. The thrust coefficient, torque coefficient, and propeller efficiency have been analyzed based on the advance ratio, as frequently used in the literature, in order to determine the propeller operating performance. The results are also discussed in terms of the spindle torque coefficient as proposed by Yurtseven and Aktay (2023).

Figure 6 shows the propeller performance coefficients for the VP1304 propeller designs with and without Duct

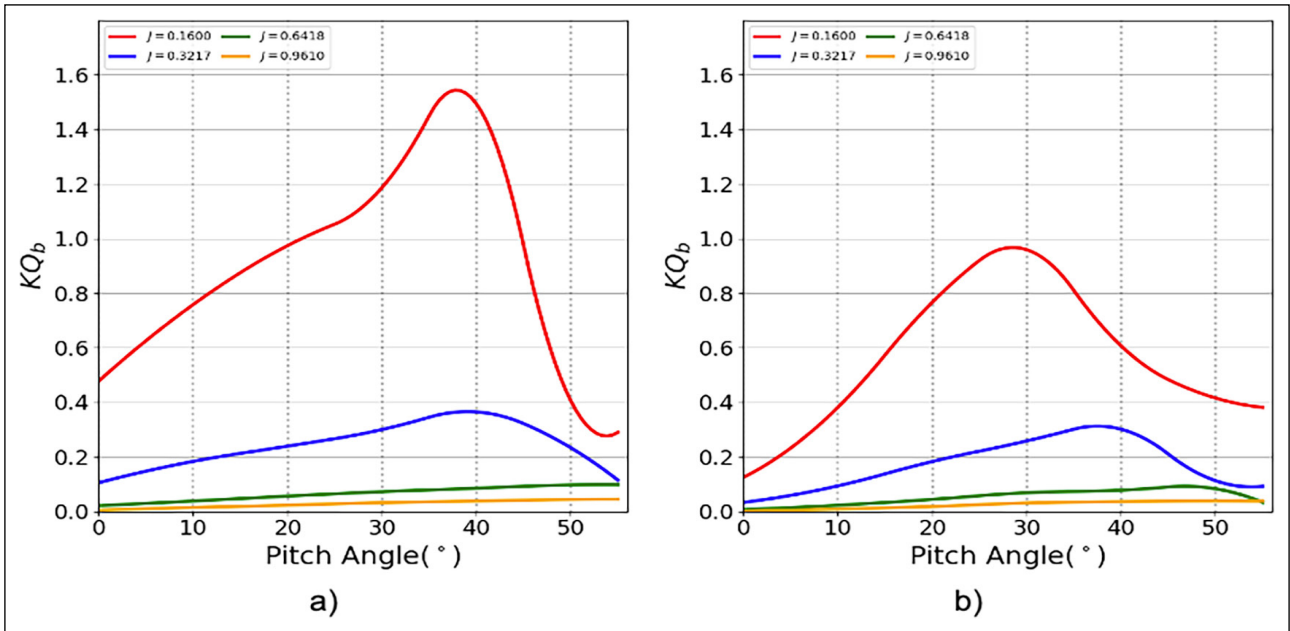


Figure 7. Spindle torque coefficient for (a) non-ducted propeller and (b) ducted propeller.

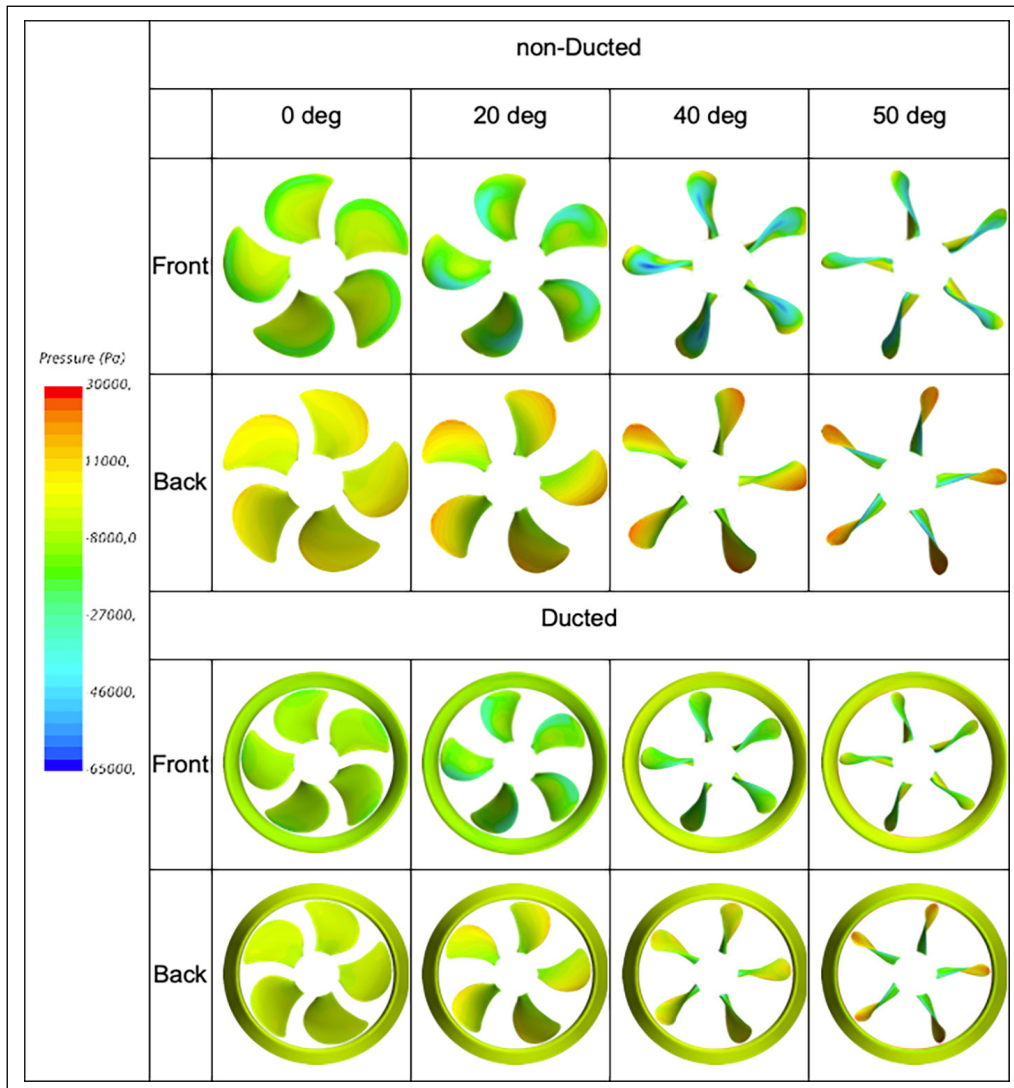


Figure 8. Upstream(front) and downstream(back) pressure distributions for non-ducted and ducted propellers ($J=0.16$).

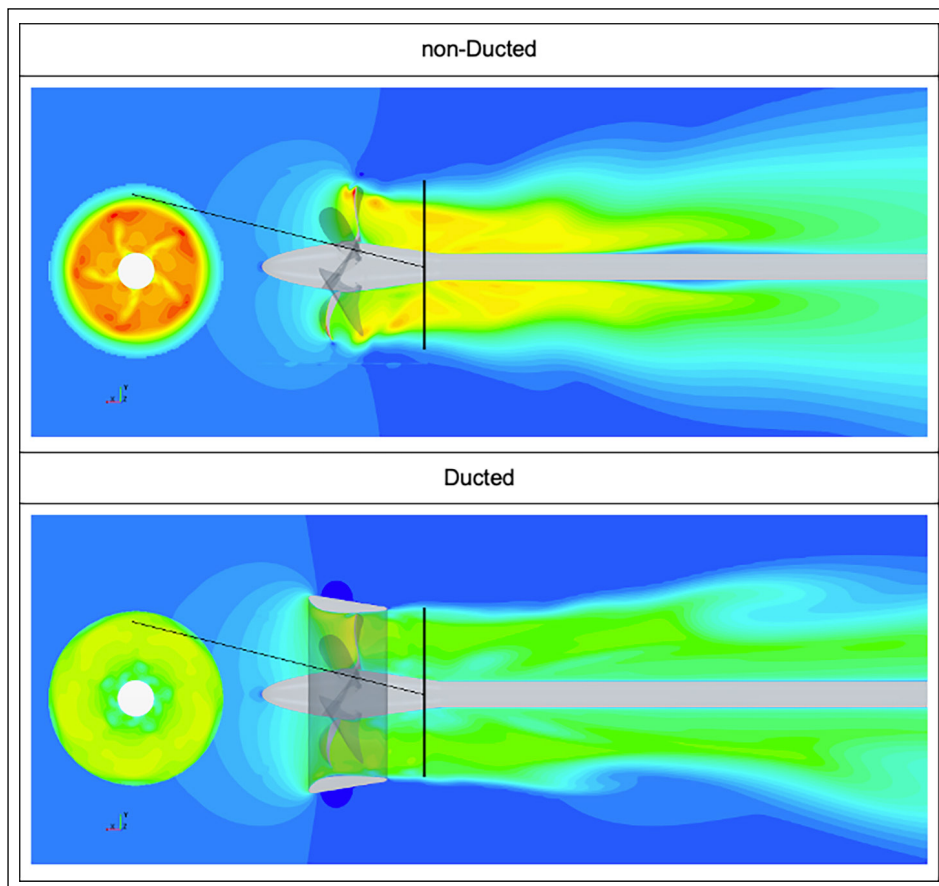


Figure 9. Velocity distributions along the longitudinal center planes of ducted and non-ducted propellers ($J=0.16$).

19A. In terms of thrust, two cases occur for the ducted propeller design. The ducted case shows the performance changes should be examined separately as those realized on the propeller itself and then the performance change on the propeller group, which can be called the ducted propeller group. An increase in the is known to decrease the propeller loading. For the ducted propeller, the thrust coefficient of the propeller alone gives lower values than the non-ducted propeller for all advance ratios. Although these values converge as the advance ratio increases, no specific high value was found. However, the thrust coefficient of the ducted propeller group gives very similar results to that for the non-ducted propeller at low advance ratios (i.e., under heavy load conditions). However, this similarity deteriorates negatively as the advance ratio increases.

In terms of propeller torque coefficient, the ducted propeller is seen to give significantly lower values, especially at low advance ratios. Therefore, it has a higher propeller efficiency than for the non-ducted propeller. However, this situation again converges to the torque coefficient of the non-ducted propeller, with the propeller efficiency decreasing significantly as the advance ratio increases.

Figure 7 gives the spindle torque coefficients for the VP1304 CPP propeller, ducted in Figure 7a and non-ducted in Figure 7b. The curves are plotted as a function of the change in blade pitch angle, with 0° indicating the design pitch of the propeller at full track and 55° indicating the feathering position.

Figure 7a shows the highest value of the blade spindle torque coefficient to be obtained at a low advance ratio. The spindle torque coefficient is seen to decrease as the advance ratio increases. Figure 7b shows the highest spindle torque coefficient in the ducted design to decrease significantly compared to the non-ducted design and to occur at a lower pitch angle. This decrease is practically insignificant after the advance ratio increases to a certain point.

Figure 8 shows the pressure distributions at different pitch angles for the front face and back face for the ducted and non-ducted propeller designs at an advance ratio of $J=0.16$. In Figure 8, the front face shows the upstream region, and the back face shows the downstream region. The ducted propeller achieves a more homogeneous pressure distribution by increasing the pressure on the front face and decreasing the pressure on the back face, especially in the regions close to the blade tips up to a 40° pitch angle. In addition, because the flow is accelerated at all angles, a general reduction in the pressure distribution is obtained on the surfaces. In this case, the ducted design reduces the overall blade spindle torque on the propellers. However, the accelerated flow shows the blades to stall much earlier when changing pitch.

Figure 9 shows the velocity distributions on the longitudinal center plane for the ducted and non-ducted propeller designs. According to these velocity distributions, the use of a duct increases the current flowing through the propeller to about 3%, thus increasing efficiency and reducing the torque on the

blade shaft axis, which allows the blade to maneuver much more effectively. In addition, the wake zone distributions shown in Figure 9 also reveal the use of the duct to correct the propeller wake, thus contributing to the increase in efficiency.

4. CONCLUSION

This study placed a standard Duct 19A nozzle as a test duct on the VP1304 propeller, provided experimental data to the VP1304 as a CPP test propeller, and then examined the change in propeller performance.

At low advance ratios (i.e., under heavy load conditions), the blade spindle torque was observed to decrease for the ducted propeller compared to the non-ducted propeller.

Because the flow is accelerated and a homogeneous distribution of the wake is obtained in the ducted propeller, the thrust values of the ducted propeller group increased at low advance ratios. At the same time, an increase in propeller efficiency was also achieved.

The blade spindle torque, which provides the movement of the blades for pitch change in CPP propellers, was observed to be significantly reduced in the ducted propeller. This reduction was also found to be more pronounced at low advance ratios, with the use of ducts also observed to cause the blades to stall earlier.

Future studies should investigate the cavitation behavior and flow-induced noise in ducted and non-ducted CPP propellers.

DATA AVAILABILITY STATEMENT

The published publication includes all graphics and data collected or developed during the study.

CONFLICT OF INTEREST

The author declared no potential conflicts of interest with respect to the research, authorship, and/or publication of this article.

ETHICS

There are no ethical issues with the publication of this manuscript.

FINANCIAL DISCLOSURE

The authors declared that this study has received no financial support.

REFERENCES

- Arief, I. S., Baidowi, A., & Ulfa, M. (2021). Thrust and torque analysis on propeller c4-40 with the addition of kort nozzle to pitch variation. *International Journal of Marine Engineering Innovation and Research*, 6(3). [\[CrossRef\]](#)
- Baltazar, J., & De Campos, J. a. C. F. (2019). Potential flow modelling of ducted propellers with blunt trailing edge duct using a panel method. *ResearchGate*. https://www.researchgate.net/publication/349253122_Potential_Flow_Modelling_of_Ducted_Propellers_with_Blunt_Trailing_Edge_Duct_Using_a_Panel_Method.
- Bhattacharyya, A., Neitzel, J. C., Steen, S., & Krasilnikov, V. (2015). Influence of flow transition on open and ducted propeller characteristics. *ResearchGate*. https://www.researchgate.net/publication/346880301_Influence_of_Flow_Transition_on_Open_and_Ducted_Propeller_Characteristics.
- Bhattacharyya, A., Krasilnikov, V. I., & Steen, S. (2016). Scale effects on open water characteristics of a controllable pitch propeller working within different duct designs. *Ocean Engineering*, 112, 226–242. [\[CrossRef\]](#)
- Bhattacharyya, A., Krasilnikov, V., & Steen, S. (2016b). A CFD-based scaling approach for ducted propellers. *Ocean Engineering*, 123, 116–130. [\[CrossRef\]](#)
- Caldas, A., Meis, M., & Sarasquete, A. (2010). CFD validation of different propeller ducts on Open Water condition. In *13th Numerical Towing Tank Symposium*, Germany.
- Celik, F., Dogrul, A., Arıkan, Y., (2011). Investigation of the optimum duct Geometry for A Passenger ferry. In: *Proceedings of the 9th Symposium on High-Speed Marine Vehicles*.
- Celik, F., Guner, M., & Ekinici, S. (2010). An approach to the design of ducted propeller. *ScientaIranica Transaction B: Mechanical Engineering*, 17(5), 406–417.
- Celik, I. B., Ghia, U., Roache, P. J., & Freitas, C. J. (2008). Procedure for estimation and reporting of uncertainty due to discretization in CFD applications. *Journal of Fluids Engineering-transactions of the Asme*, 130(7), Article 078001. [\[CrossRef\]](#)
- Cosner, R., Oberkampf, B., Rumsey, C., Rahaim, C., & Shih, T. (2006). AIAA Committee on standards for computational fluid dynamics: status and plans. *44th AIAA Aerospace Sciences Meeting and Exhibit*. [\[CrossRef\]](#)
- Elbatran, A. H., Kotb, M. A., Hassan, A. A., Ahmed, M. W. A. E., & Banawan, A. A. (2014). Stationary and low speed performance characteristics of open and ducted CPPs. *ResearchGate*. https://www.researchgate.net/publication/301777898_Stationary_and_Low_Speed_Performance_Characteristics_of_Open_and_Ducted_CPPs.
- Funeno, I., Pouw, C., & Bosman, R. (2013). Measurements and computations for blade spindle torque of controllable pitch propellers in open water. In *Proceedings of the Third International Symposium on Marine Propulsors (SMP; Vol. 13)*.
- Godjevac, M., Van Beek, T., Grimmelius, H. T., Tinga, T., & Stapersma, D. (2009). Prediction of fretting motion in a controllable pitch propeller during service. *Proceedings of the Institution of Mechanical Engineers, Part M: Journal of Engineering for the Maritime Environment*, 223(4), 541–560. [\[CrossRef\]](#)
- Gong, J., Ding, J., & Wang, L. (2021). Propeller-duct interaction on the wake dynamics of a ducted propeller. *Physics of Fluids*, 33(7), Article 074102. [\[CrossRef\]](#)

- Haimov, H., Vicario, J., & Del Corral, J. (2011). RANSE code application for ducted and endplate propellers in open water. In *Proceedings of the Second International Symposium on Marine Propulsors* (pp. 1–9).
- Heinke, H. J. (2011). Potsdam Propeller Test Case (PPTC), Open Water Tests with the Model Propeller, VP1304, *Second International Symposium on Marine Propulsors smp'11, Hamburg, Germany*, Report 3753.
- Huisman, J., Garenaux, M., de Jager, A., & Janse, G. (2022). Validation of Cavitation Prediction of Ducted Propeller Design and Analysis Tools. *Seventh International Symposium on Marine Propulsors (SMP'22)*, Wuxi, China.
- International Towing Tank Conference. (1999). Recommended Procedures and Guidelines-CFD, General CFD Verification. *International Towing Tank Conference* <https://www.itc.info/media/8153/75-03-01-01.pdf>.
- Kajitani, H., Miyata, H., Ikehata, M., Tanaka, H., Adachi, H., Namimatsu, M., Ogiwara, S. (1983). *The Summary of the Cooperative Experiment on Wigley Parabolic Model in Japan the Executive Members 4 I*. <https://apps.dtic.mil/sti/tr/pdf/ADP003037.pdf>.
- Jessup, S. (2009). *Measurements of controllable pitch propeller blade loads under cavitating conditions*. <https://www.semanticscholar.org/paper/Measurements-of-Controllable-Pitch-Propeller-Blade-Jessup-Donnelly/b0ee4866632d2428b4d33c8ee166c8f852328737>.
- Kim, K. W., Paik, K. J., Lee, J. H., Song, S. S., Atlar, M., & Demirel, Y. K. (2021). A study on the efficient numerical analysis for the prediction of full-scale propeller performance using CFD. *Ocean Engineering*, 240, Article 109931. [CrossRef]
- Kim, S., & Kinnas, S. A. (2022). A panel method for the prediction of unsteady performance of ducted propellers in ship behind condition. *Ocean Engineering*, 246, Article 110582. [CrossRef]
- Liu, A., Dang, J., Xie, Q., & Hu, J. (2015). The effect of sheet cavitation on the blade spindle torque of a controllable pitch propeller. In *4th International Symposium on Marine Propulsors*.
- Liu, X. L., & Wang, G. Q. (2006). A potential based panel method for prediction of steady performance of ducted propeller. *Journal of Ship Mechanics*, 10(6), 26–35.
- Martelli, M., Figari, M., Altosole, M., & Vignolo, S. (2014). Controllable pitch propeller actuating mechanism, modelling and simulation. *Proceedings of the Institution of Mechanical Engineers, Part M: Journal of Engineering for the Maritime Environment*, 228(1), 29–43. [CrossRef]
- Oosterveld, M. W. C. (1972). Ducted propeller systems suitable for tugs and pushboats. *International Shipbuilding Progress*, 19(219), 351–371. [CrossRef]
- Pourmostafa, M., & Ghadimi, P. (2020). Applying boundary element method to simulate a high-skew Controllable Pitch Propeller with different hub diameters for preliminary design purposes. *Cogent Engineering*, 7(1), Article 1805857. [CrossRef]
- Roache, P. J. (1994). Perspective: a method for uniform reporting of grid refinement studies. *Journal of Fluids Engineering-transactions of the Asme*, 116(3), 405–413. [CrossRef]
- Siemens, DISW. (2021). *Star CCM+ Version 2020.3. User guide*. n.d. <https://community.sw.siemens.com/s/question/0D54O000061xpUOSAY/simcenter-starccm-user-guide-tutorials-knowledge-base-and-tech-support>
- Tarbiat, S., Ghassemi, H., & Fadavie, M. (2014). Numerical prediction of hydromechanical behaviour of controllable pitch propeller. *International Journal of Rotating Machinery*, 2014, Article 180725. [CrossRef]
- Yurtseven, A., & Aktay, K. (2023). The numerical investigation of spindle torque for a controllable pitch propeller in feathering maneuver. *Brodogradnja: Teorija I praksa brodogradnje I pomorske tehnike*, 74(2), 95–108. [CrossRef]
- Zhang, Q., & Jaiman, R. K. (2019). Numerical analysis on the wake dynamics of a ducted propeller. *Ocean Engineering*, 171, 202–224. [CrossRef]
- Zhang, Q., Jaiman, R. K., Ma, P., & Liu, J. (2020). Investigation on the performance of a ducted propeller in oblique flow. *Journal of Offshore Mechanics and Arctic Engineering*, 142(1), Article 011801. [CrossRef]
- Zhang, T., & Barakos, G. N. (2021). High-fidelity numerical analysis and optimisation of ducted propeller aerodynamics and acoustics. *Aerospace Sci Technol* 113, Article 106708. [CrossRef]